

## $\beta$ -Induced Alfvén Eigenmodes Destabilized by Energetic Electrons in a Tokamak Plasma

W. Chen,\* X. T. Ding, Q. W. Yang, Yi Liu, X. Q. Ji, Y. P. Zhang, J. Zhou, G. L. Yuan, H. J. Sun, W. Li, Y. Zhou, Y. Huang, J. Q. Dong, B. B. Feng, X. M. Song, Z. B. Shi, Z. T. Liu, X. Y. Song, L. C. Li, X. R. Duan, Y. Liu, and HL-2A team

*Southwestern Institute of Physics, P.O. Box 432 Chengdu 610041, China*

(Received 10 June 2010; published 26 October 2010)

The  $\beta$ -induced Alfvén eigenmode (BAE) excited by energetic electrons has been identified for the first time both in the Ohmic and electron cyclotron resonance heating plasma in HL-2A. The features of the instability, including its frequency, mode number, and propagation direction, can be observed by magnetic pickup probes. The mode frequency is comparable to that of the continuum accumulation point of the lowest frequency gap induced by the shear Alfvén continuous spectrum due to finite  $\beta$  effect, and it is proportional to Alfvén velocity at thermal ion  $\beta$  held constant. The experimental results show that the BAE is related not only with the population of the energetic electrons, but also their energy and pitch angles. The results indicate that the barely circulating and deeply trapped electrons play an important role in the mode excitation.

DOI: 10.1103/PhysRevLett.105.185004

PACS numbers: 52.35.Bj, 52.55.Pi

Alfvénic instabilities can be driven by the energetic particle in future burning plasma devices, such as ITER and DEMO, where energetic particles will be abundantly produced by high power heating and fusion reaction. These instabilities can lead to significant loss of fast particles, which are very harmful for plasma heating and reactor's first wall. So it is very important to study them theoretically and experimentally in present-day tokamak plasmas. The instabilities driven by fast ions, such as toroidicity-induced Alfvén eigenmodes (TAEs), have been observed and investigated widely in many fusion devices [1]. In contrast, the modes related to energetic electrons are much less explored. Understanding of energetic-electron behaviors can provide a strong contribution to clarify physics of burning plasma behaviors because their effect on low-frequency MHD modes can be used to simulate and analyze the analogous effect of  $\alpha$  particles characterized by small dimensionless orbits similar to energetic electrons in present-day tokamak plasmas [2].

The  $\beta$ -induced Alfvén eigenmodes (BAEs) were first observed in DIII-D and then TFTR plasmas with fast ions [3–5]. Subsequently, the BAEs (termed as m-BAEs; here the “m” denotes that the BAEs are excited by magnetic islands) have also been observed during a strong tearing mode (TM) activity in FTU and TEXTOR Ohmic plasmas without fast ions [6–8]. Recently, the BAEs have also been reported during a sawtooth cycle in ASDEX-U and TORE-SUPRA plasmas with fast ions [9,10]. The detailed excitation mechanism of the BAEs is still not fully assessed due to many effects, such as ion diamagnetic drift, thermal ion compression, finite Larmor radius or finite orbit width, and energetic-particle effects. In this work, we discuss for the first time experimental observations of BAEs (termed as e-BAEs) destabilized by energetic electrons in the Huan-Liuqi-2A (HL-2A) tokamak, and a comparative analysis of e-BAEs and m-BAEs is also presented in this Letter.

HL-2A is a medium-size tokamak with major radius  $R = 1.65$  m and minor radius  $a = 0.4$  m. The experiments discussed here were performed in deuterium plasmas with toroidal plasma current  $I_p = 160/300$  kA, toroidal field  $B_t = 1.3/2.4$  T, safety factor at the edge  $q_a \approx 4.0$ , and electron cyclotron resonance heating (ECRH) as the main heating. The line averaged density was detected by a hydrogen cyanide interferometer. The electron and ion temperature were measured by the Thomson laser scattering and neutral particle analyzer, respectively. The hard-x-ray spectrum detected by cadmium-telluride (CdTe) and the nonthermal radiation measured by the electron cyclotron emission (ECE) were used to analyze the behaviors of the energetic electrons.

*Mode characteristics.*—The e-BAE has been observed in the HL-2A ECRH plasma. This phenomenon is perfectly reproducible. The mode features, including its frequency, mode number, and propagation direction, can be observed by magnetic pickup probes. The observed mode activity exhibits no amplitude bursting or frequency chirping, different from electron fishbone characteristics in HL-2A [11,12]. The mode frequency is comparable to that of the continuum accumulation point (CAP) of the lowest frequency gap induced by the shear Alfvén continuous spectrum due to finite  $\beta$  effect [13]. Figure 1 shows a typical experimental result with low plasma density during ECRH. Electron cyclotron wave (1 MW, 68 GHz, second harmonic heating) was launched into the plasma with 1.3 T toroidal magnetic field. Here, the plasma density, ECRH pulse, neutral-beam injection (NBI) pulse, magnetic fluctuation signal from Mirnov probes, and its frequency spectrum are shown from the top to the bottom. A coherent MHD fluctuation is visible around 20 kHz between 420 and 800 ms. The density slightly increases after NBI at  $t = 550$  ms, but the mode remains almost unchanged. The mode becomes very weak after ECRH switched off at  $t = 800$  ms,

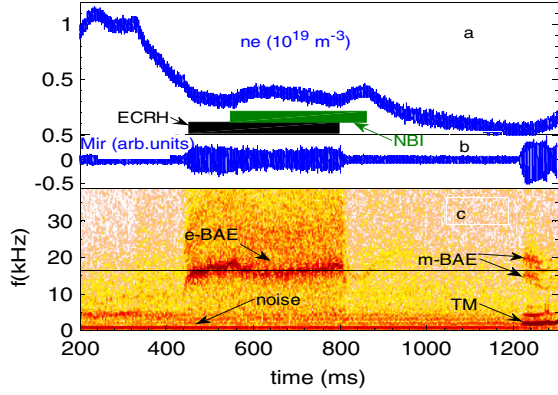


FIG. 1 (color online). HL-2A pulse no. 10579. (a) Central line-average density, (b) magnetic probe signal, (c) the spectrogram of magnetic probe signal. Plasma current  $I_p = 160$  kA, toroidal field  $B_t = 1.3$  T, central ion and electron temperature  $T_i \sim 0.85$  keV,  $T_e \sim 1.10$  keV, edge safety factor  $q_a \approx 4.0$ , ECRH power  $P_{\text{ECRH}} = 1.0$  MW, off-axis heating at LFS and NBI power  $P_{\text{NBI}} = 0.38$  MW.

although NBI presents at  $t = 800\text{--}860$  ms. These fluctuations do not correspond to TAEs because their frequencies are much smaller than TAE frequency  $f_{\text{TAE}} = v_A/4\pi qR$  ( $f_{\text{TAE}} \approx 160$  kHz for the deuterium plasma with  $B_t = 1.3$  T,  $n_e = 0.4 \times 10^{19} \text{ m}^{-3}$ , and  $q = 3$  in HL-2A). The magnetic field fluctuations measured at the wall are  $\delta B_\theta/B \sim 10^{-5}\text{--}10^{-4}$  and have clear mode numbers  $m/n = -3/-1$ . The m-BAEs were also visible during strong TM activity in the same discharge. The characteristics of the m-BAEs were investigated in previous works [14], and the new theoretic explanation for the m-BAEs was presented recently in Ref. [15]. The mode numbers of the m-BAEs are  $m/n = 2/1$  and  $-2/-1$ . The m-BAEs propagate poloidally and toroidally in opposite directions and form standing-wave structures in the island rest frame. There exists an island width threshold for the m-BAEs excitation. The mode frequencies shift with respect to the BAE CAP, and are proportional to the magnetic island width. When comparing with two cases, it is found that the frequency of  $m/n = -3/-1$  mode is of the same order of the frequencies of the m-BAEs. The  $m/n = -3/-1$  mode propagates poloidally parallel to the electron diamagnetic drift velocity and toroidally opposite to the plasma current direction in the laboratory frame of reference.

*Mode excited by energetic electrons.*—Figure 2 shows that the mode can also be observed at higher density and toroidal magnetic field. In this discharge, the mode can be found when the density is around  $n_e \approx 1.6 \times 10^{19} \text{ m}^{-3}$  with toroidal magnetic field  $B_t = 2.4$  T, but the mode intensity is very weak. Figure 2 also shows that the  $m/n = -3/-1$  mode excitation is correlated with the energetic electrons. The energy distribution of the electrons was indirectly measured by a hard-x-ray detector (CdTe) with the pulse height analysis. The counts of hard-x-ray photons increase largely during ECRH, and they are shown in Figs. 2(a)–2(c). When the counts of the energetic electrons

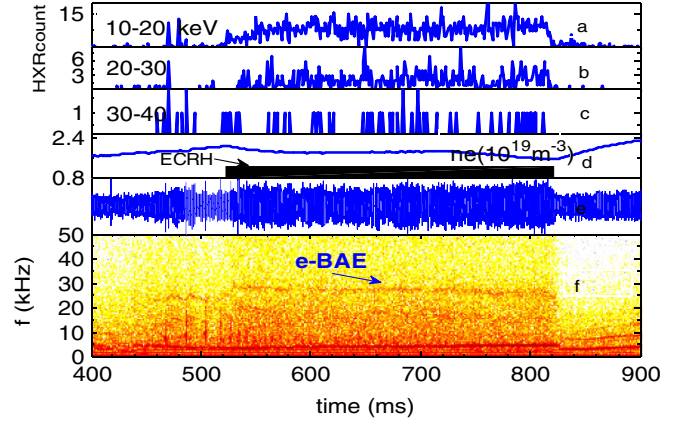


FIG. 2 (color online). HL-2A pulse no. 13364. (a)–(c) Counts of hard-x-ray (HXR) photons at different energy ranges, (d) central line-average density, (e) magnetic probe signal, (f) the spectrogram of magnetic probe signal. Plasma current  $I_p = 320$  kA, toroidal field  $B_t = 2.4$  T, central electron temperature,  $T_e \sim 2.3$  keV, edge safety factor  $q_a \approx 4.0$ , and ECRH power  $P_{\text{ECRH}} = 1.41$  MW, on-axis heating.

with 10–40 keV increase to a higher level, the  $m/n = -3/-1$  mode is observed. From Figs. 1 and 2 it is found that the energetic electrons produced by EC wave can provide the necessary energy to drive modes when the stability threshold is exceeded during ECRH. The population of energetic electrons is insufficient for mode excitation after ECRH is switched off, and cannot overcome damping. The off-axis ECRH power deposited on the lower field side (LFS), which suggests that the deeply trapped electrons predominantly contribute to the mode excitation.

The  $m/n = -3/-1$  mode can often be observed in low density Ohmic plasma. From Fig. 3, it is found that the intensity of the mode in Ohmic plasma is weak at  $t = 600\text{--}1200$  ms, but it becomes strong during high power ECRH in the same discharge. It can be shown that the  $m/n = -3/-1$  mode in Ohmic plasma is also excited by energetic electrons. It is well known that the electrons can be accelerated by the Ohmic electric field in tokamak plasma. Under the influence of the longitudinal electric field, the initially Maxwellian electron distribution function begins to grow an energetic-electron tail. The low density discharge regime is characterized by a large supra-thermal electron population. When the ratio of the electron plasma frequency to the electron cyclotron frequency  $\omega_{pe}/\omega_{ce} < 0.3$  according to the empirical values in several machines, the anomalous Doppler instability (ADI) can be excited [16–19]. For no. 10580 discharge with toroidal field  $B_t = 1.3$  T, the ADI is excited when the density is less than critical density  $n_{ec} \approx 0.14 \times 10^{19} \text{ m}^{-3}$ . From Fig. 3, it is found that the  $m/n = -3/-1$  mode disappears as soon as the ADI is excited at  $t = 1200$  ms. The ADI causes pitch angle scattering of the energetic electrons. The ADI transfers energy from parallel to perpendicular motion; i.e., the circulating electrons become the barely trapped electrons primarily. This suggests that

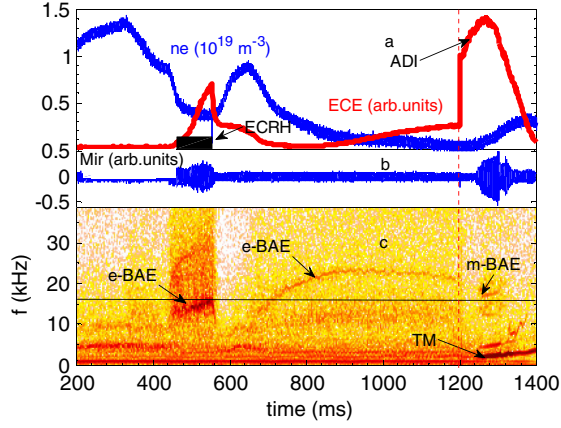


FIG. 3 (color online). HL-2A pulse no. 10580. (a) Central line-average density and nonthermal radiation measured by ECE, (b) magnetic probe signal, (c) the spectrogram of magnetic probe signal. Plasma current  $I_p = 160$  kA, toroidal field  $B_t = 1.3$  T, central ion and electron temperature  $T_i \sim 0.50$  keV,  $T_e \sim 0.62$  keV, edge safety factor  $q_a \approx 4.0$ , and ECRH power  $P_{\text{ECRH}} = 0.89$  MW, off-axis heating at LFS.

the circulating energetic electrons also effectively contribute to the mode excitation.

*Frequency scaling.*—A linear scaling on the toroidal magnetic field  $B_t$  and line-average density  $ne$  is shown in Fig. 4. It is evident that the mode frequency is proportional to Alfvén velocity in both the Ohmic and ECRH plasma, i.e.,  $f \propto B_t/ne^{1/2} \propto v_A$ , similar to analogous scalings reported in Refs. [6,7], indicating that the  $m/n = -3/-1$  mode is most likely a kind of shear Alfvén eigenmode. Note that the scaling with the Alfvén speed is consistent with the dependence of the BAE-CAP frequency with the thermal ion transit frequency, provided that the thermal ion  $\beta$  is held constant, as it is adequately done in our case. The scaling relation is shown in the case of  $I_p = 160$  kA and  $B_t \sim 1.3$  T to avoid spurious dependences on other effects, e.g., plasma rotation.

*Calculation and analysis.*—To identify the  $m/n = -3/-1$  mode with the BAE on HL-2A, the generalized fishbonelike dispersion relation (GFLDR) developed by Zonca has been solved near marginal stability [2,13,20–23]. The GFLDR is used to study plasma

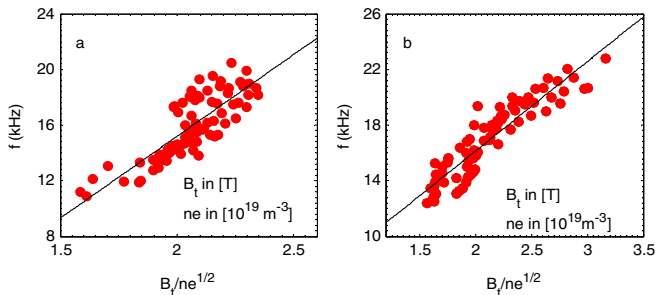


FIG. 4 (color online). The mode frequencies versus the Alfvén velocity. (a) ECRH plasma, (b) Ohmic plasma. Marker point (●) denotes raw data. Solid line denotes linear fit result.

dynamics with the frequency range from kinetic ballooning mode (KBM)/BAE to TAE. The GFLDR can be given by

$$-i\Lambda(\omega) + \delta\hat{W}_f + \delta\hat{W}_k = 0, \quad (1)$$

where  $i\Lambda(\omega)$  is the inertial layer contribution due to thermal ions, while  $\delta\hat{W}_f$  and  $\delta\hat{W}_k$  come from fluid MHD and energetic-particle contributions in the regular ideal regions. The frequency gap of shear Alfvén wave (SAW) can be given by the condition  $\text{Re}\Lambda^2 < 0$ . On the basis of the GFLDR, the two types of modes exist. One is the discrete AE for  $\text{Re}\Lambda^2 < 0$ . Another one is the EPM for  $\text{Re}\Lambda^2 > 0$ . The combined effect of  $\delta\hat{W}_f$  and  $\text{Re}\delta\hat{W}_k$  determines the existence conditions of AE by removing the degeneracy with the SAW accumulation point, and it depends on the plasma equilibrium profiles, e.g., temperature, density, and safety factor. Thus, the various effects on  $\delta\hat{W}_f + \text{Re}\delta\hat{W}_k$  can lead to AE localization in various gaps, i.e., to different types of AE [23]. When considering the kinetic effects on low mode number MHD modes, the sideband poloidal mode numbers cannot be considered degenerate and the kinetic expression of  $\Lambda$  for  $\omega_{bi} < |\omega| \ll \omega_A$  is given by [23]

$$\Lambda^2 = \frac{\omega^2}{\omega_A^2} \left(1 - \frac{\omega_{*pi}}{\omega}\right) + q^2 \frac{\omega \omega_{ti}}{\omega_A^2} \left[ \left(1 - \frac{\omega_{*ni}}{\omega}\right) F - \frac{\omega_{*Ti}}{\omega} G - \frac{N_m}{2} \left(\frac{N_{m+1}}{D_{m+1}} + \frac{N_{m-1}}{D_{m-1}}\right) \right], \quad (2)$$

where  $\omega_{*pi} = \omega_{*ni} + \omega_{*Ti} = (T_i/eB)k_\theta(\nabla \ln n_i)(1 + \eta)$  is ion diamagnetic drift frequency,  $\omega_{*ni} = (T_i c/eB)(\vec{k} \times \vec{b}) \cdot \nabla \ln n_i$ ,  $\omega_{*Ti} = (T_i c/eB)(\vec{k} \times \vec{b}) \cdot \nabla \ln T_i$ ,  $\eta = \nabla \ln T_i / \nabla \ln n_i$ ,  $k_\theta = -m/r$ , and  $\omega_{Ti}$  is ion transit frequency, and the functions,  $F(x)$ ,  $G(x)$ ,  $N(x)$ , and  $D(x)$  are given by Ref. [23], and all symbols are standard.  $N_m(x)$  and  $D_m(x)$  are defined as the functions  $N(x)$  and  $D(x)$ , having made explicit the poloidal mode number  $m$  to be used for computing their dependences on diamagnetic frequencies. The thermal ion transit resonances as well as diamagnetic effects (finite  $\omega_{*pi}$ ) usually provide higher order corrections to the frequency spectrum.

On the basis of experimental measurements and EFIT equilibrium reconstruction, we assume  $B = 1.3$  T, and  $r = 32$  cm,  $n_e = n_i$ ,  $\eta = 1.5$ , and  $-R_0 \nabla \ln n_i = 6.0$  at the  $q = 3$  surface. We obtain  $k_\theta = m/32$  cm  $\approx m \times 3.1$  m $^{-1}$  and  $\omega_{*pi}/2\pi = (\omega_{*ni} + \omega_{*Ti})/2\pi \approx mT_i \times 3.5$  kHz. According to the parameters, Eq. (2) has been solved near marginal stability ( $\Lambda = 0$ ). Figure 5 shows the frequency of the BAE accumulation point versus ion temperature at  $q = 3$  surface. Using pulse no. 10579 experimental data, the ion diamagnetic frequency is  $\omega_{*pi}/2\pi \approx 1.6$  kHz at the  $q = 3$  surface with  $T_i|_{q=3} \approx 0.15$  keV. The observed frequency of the  $m/n = -3/-1$  mode is around  $f = 18$  kHz, while the frequency of the BAE accumulation point is around  $f \approx 19$  kHz ( $\tau = 1$ ) or  $f \approx 22$  kHz ( $\tau = 2$ ). It is obvious that the observed frequency coincides with the theoretical prediction based on the GFLDR. This result, along with the

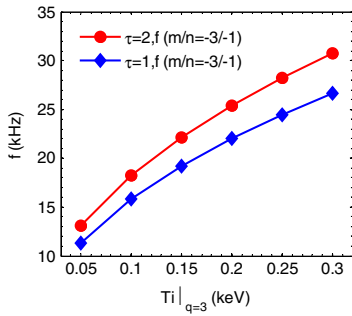


FIG. 5 (color online). The frequency of the BAE accumulation point versus ion temperature at  $q = 3$  surface.  $\tau = T_e/T_i$ .

experimental evidence reported above, supports the conclusion that the mode is the e-BAE instability.

In an idealized case of uniform magnetic field, the wave particle resonance condition requires the electron velocity along the magnetic field  $v_{\parallel}$  to be equal to the wave phase velocity  $v_p = \omega/k_{\parallel}$ . Wave-particle interaction of energetic electrons at the precession frequency was originally considered in Ref. [24] and proposed as a mechanism to drive energetic-particle instabilities. The fishbone activities were explained with the same kind of precession drift instability due to energetic ions [20] or electrons [25]. Our experimental result has indicated that the e-BAE is driven by the barely circulating electrons or deeply trapped electrons. The barely circulating electron as well as deeply trapped electron has an effect on  $\delta\hat{W}_k$  when the magnetic shear is positive. For the circulating electrons ( $0 < \kappa^2 < 1$ ) and trapped electrons ( $\kappa^2 > 1$ ), the averaged precession frequency  $\bar{\omega}_d$  can be given using the  $(s, \alpha)$  model tokamak equilibrium [2]. For  $B_t = 1.3/2.4$  T,  $E = 35$  keV,  $(s, \alpha) = (1.5, 1)$ ,  $r = 0.32$  m, and  $\kappa^2 = 0.6$ , the precession frequency of barely circulating electron is  $f_d \approx 15$ –20 kHz. For  $B_t = 1.3/2.4$  T,  $E = 35$  keV,  $(s, \alpha) = (1.5, 1)$ ,  $r = 0.32$  m, and  $1/\kappa^2 = 0.3$ , the precession frequency of deeply trapped electron is  $f_d \approx 13$ –20 kHz. These are clearly close to the observed frequencies. This calculation result supports that conclusion that the e-BAE is excited by the barely circulating electrons or deeply trapped electrons.

In summary, the experimental data presented here identify for the first time an energetic-electron-driven BAE in HL-2A. The e-BAE and m-BAE often can be observed in the same discharge, and their frequencies are similar; i.e.,  $O(f_{e\text{-BAE}}) = O(f_{m\text{-BAE}})$ . The experimental results show that the e-BAE excitation is related not only with the population of the energetic electrons, but also their energy and pitch angle. The observed mode features agree with the predictions of the GFLDR. The mode frequency is com-

parable with that of the BAE CAP of the lowest frequency gap induced by the shear Alfvén continuous spectrum due to finite  $\beta$  effect. The mode frequency is proportional to Alfvén velocity at fixed thermal ion  $\beta$ . The modes occur in plasmas with magnetic safety factor  $q = 3$  and propagate poloidally in electron diamagnetic direction.

One of the authors (C. W.) sincerely thanks Dr. F. Zonca for the inspiring lectures at Zhejiang University and acknowledges him and Dr. G. Fu for constructive comments. This work was supported by NNSF of China under Grants No. 11005035, No. 10975049, No. 10775041, No. 10775045, and No. 10775004.

\*chenw@swip.ac.cn

- [1] A. Fasoli *et al.*, *Nucl. Fusion* **47**, S264 (2007).
- [2] F. Zonca *et al.*, *Nucl. Fusion* **47**, 1588 (2007).
- [3] W. W. Heidbrink *et al.*, *Phys. Rev. Lett.* **71**, 855 (1993).
- [4] R. Nazikian *et al.*, *Phys. Plasmas* **3**, 593 (1996).
- [5] W. W. Heidbrink *et al.*, *Phys. Plasmas* **6**, 1147 (1999).
- [6] P. Buratti *et al.*, *Nucl. Fusion* **45**, 1446 (2005).
- [7] O. Zimmermann *et al.*, in *Proceedings of the 32nd EPS Conference on Plasma Physics and Controlled Fusion, Tarragona, Spain, 2005*, p. 4.059, [http://epsppd.epfl.ch/Tarragona/pdf2/P4\\_059.pdf](http://epsppd.epfl.ch/Tarragona/pdf2/P4_059.pdf).
- [8] S. V. Annibaldi *et al.*, *Plasma Phys. Controlled Fusion* **49**, 475 (2007).
- [9] C. Nguyen *et al.*, *Plasma Phys. Controlled Fusion* **51**, 095002 (2009).
- [10] P. Lauber *et al.*, *Plasma Phys. Controlled Fusion* **51**, 124009 (2009).
- [11] W. Chen *et al.*, *Nucl. Fusion* **49**, 075022 (2009).
- [12] W. Chen *et al.*, *Nucl. Fusion* **50**, 084008 (2010).
- [13] F. Zonca *et al.*, *Plasma Phys. Controlled Fusion* **38**, 2011 (1996).
- [14] W. Chen *et al.*, *J. Phys. Soc. Jpn.* **79**, 044501 (2010).
- [15] A. Biancalani *et al.*, *Phys. Rev. Lett.* **105**, 095002 (2010).
- [16] H. Knoepfel and D. A. Spong, *Nucl. Fusion* **19**, 785 (1979).
- [17] S. C. Luckhardt *et al.*, *Phys. Fluids* **30**, 2110 (1987).
- [18] P. Blanchard *et al.*, *Plasma Phys. Controlled Fusion* **44**, 2231 (2002).
- [19] H. W. Hu *et al.*, *Phys. Scr.* **81**, 025503 (2010).
- [20] L. Chen, R. B. White, and M. N. Rosenbluth, *Phys. Rev. Lett.* **52**, 1122 (1984).
- [21] F. Zonca *et al.*, *Plasma Phys. Controlled Fusion* **40**, 2009 (1998).
- [22] S. Briguglio *et al.*, *Nucl. Fusion* **40**, 701 (2000).
- [23] F. Zonca *et al.*, *Nucl. Fusion* **49**, 085009 (2009).
- [24] H. P. Furth, *Phys. Fluids* **8**, 2020 (1965).
- [25] K. L. Wong *et al.*, *Phys. Rev. Lett.* **85**, 996 (2000).